Effect of anion of polyoxometalate based organic–inorganic hybrid material on intumescent flame retardant polypropylene

Ting Ye and Juan Li*

In this work, 12-tungestocobaltic acid based organic–inorganic hybrid material, $[Bmim]_6CoW_{12}O_{40}$ (CoW) was synthesized and applied as a synergist in polypropylene (PP)/intumescent flame retardant (IFR) composites. The flame retardant properties were investigated by the limiting oxygen index (LOI), UL-94 vertical burning test, thermal gravimetric analyzer (TGA), cone calorimeter and scanning electron microscopy (SEM) etc. The results showed that the PP composites with 16 wt% IFR and 1 wt% CoW achieves the UL-94 V-0 rating and gets a LOI value 28.0. However, only add no less than 25 wt% single IFR, can the PP composites obtain the UL-94 V-0 rating, which suggests that CoW has good synergistic effects on flame retardancy of PP/IFR composites. In addition, the SEM and cone calorimeter tests indicated the CoW improves the quality of char layer. The rate of char formation has been enhanced also because of the existence of CoW. It is the combination of a better char quality and a high rate of char formation promoted by CoW that results in the excellent flame retardancy of PP/IFR composites.

Keywords: organic–inorganic hybrid material; tungestocobaltic acid; intumescent flame retardant; synergistic; polypropylene

INTRODUCTION

Polypropylene (PP) is one of the most popular thermoplastic materials because of its good chemical resistance, easy processing, low toxicity and excellent cost performance. However, the application of PP causes some potential safety hazards in many fields because of its flammable performance [1]. So, it is necessary to improve the flame retardant ability of PP. In the past several decades, researchers tried to solve this problem by introducing flame retardant element into PP via copolymerizing, grafting or blending [2–4]. Adding flame retardants into PP is a common and convenient method to decrease the flammability of PP composites compared with other ways [5,6].

With the development of technology, sustainability of flame retardant materials attracts more and more attentions. Intumescent flame retardant (IFR) is a kind of environment friendly flame retardants. It is usually composed of three parts: acid source, carbon source and blowing agent [7]. Ammonium polyphosphate (APP) and pentaerythritol (PER) are usually used as acid source and carbon source in PP, respectively. However, the flame retardant efficiency of APP/PER is not satisfied. Generally, in order to pass the UL-94 V-0 testing, no less than 25 wt% APP/PER is needed. Too much addition of flame retardants would decrease the mechanical properties of PP and rise its price. So it is pressing to improve the flame retardant efficiency of APP/PER in PP composites.

In fact, many researchers are looking for new strategies to improve the efficiency of IFR. For example, Ke et al. [8] synthesized a hyperbranched polyamine charring agent (HPCA) containing triazine and found that the IFR system containing HPCA and APP has a high efficiency in enhancing flame retardant and anti-dripping properties. Chen et al. [9] used tris(2-hydroxyethyl) isocyanurate (THEIC) as charring agent to modify the flame

retardant property of PP. Wang et al. [10] synthesized a novel and efficient halogen-free composite flame retardant by brucite and zinc borate, and proved its good flame retardant performance. These works promote the development of IFR technology greatly. However, developing a novel IFR usually needs long time; introducing catalysts or synergists into commercial APP/PER system is a simple and convenient method. Based on the mechanism of IFR: APP would react with PER to form esters, and then turn into char at high temperature during combustion [11–16]. The rate of esterification, char formation and char quantity are the most important factors for improving flame retardancy. Many catalysts or synergists which promote the esterification were chosen to modify the flame retardancy of APP/PER in PP, such as metallic oxide, metallic salt and solid acid [17–20]. The results showed that these additives increase the flame retardancy of PP/APP/PER in a certain extent. However, the development of flame retardant technology has no end. More efficient catalysts or synergists need to be found to improve the flame efficiency of IFR in PP and to meet the requirements of new rules and technologies.

Recently, organic–inorganic hybrid compound based on phosphomolybdic acid (PMo) and 1-butyl-3-methylimidazolium (Bmim) was used in PP/APP/PER system and achieved a great improvement on flame retardant efficiency [21]. Only containing 0.5 wt% $[Bmim]_3PMo$ and 14.5 wt% APP/PER, the PP composites

* Correspondence to: Juan Li, Ningbo Key Laboratory of Polymer Materials, Ningbo Institute of Material Technology and Engineering, Chinese Academy of Sciences, Ningbo, Zhejiang 315201, PR China. E-mail: lijuan@nimte.ac.cn

T. Ye, J. Li
Ningbo Key Laboratory of Polymer Materials, Ningbo Institute of Material Technology and Engineering, Chinese Academy of Sciences, Ningbo, Zhejiang, 315201, PR China

can pass the UL-94 V-0 testing. However, the color of PP/IFR composites would turn to dark brown with the addition of [Bmim]$_3$PMo. The color of materials is very important for industrial applications. In addition, the used anion and cation of [Bmim]$_3$PMo are both expensive. So it is highly necessary to find more organic and inorganic parts to tailor the performance of polyoxometalates and to regulate its color and price further.

In this work, we chose cobalt (Co) as the heteroatom to tailor the performance of polyoxometalates. [Bmim]$_6$CoW$_{12}$O$_{40}$ (CoW) was synthesized and used as synergist. PP composites were prepared by using APP/PER (3:1 wt%/wt%) as IFR and CoW as synergist. The limiting oxygen index (LOI), UL-94 vertical burning test, thermal gravimetric analyzer (TGA) and cone calorimeter were used to investigate the flame retardancy and the reaction mechanism in PP composites. The scanning electron microscopy (SEM) was also applied to observe the morphology of char residues of PP composites after combustion.

EXPERIMENTAL

Materials

PP resin (F401, melt flow rate: 2.0 g/10 min) was purchased from Yangzi Oil Company (Shanghai China). APP (231, $n > 1500$) was supplied by Presafer Phosphor Chemical Company Limited (Qingyuan, China). PER was purchased from Aladdin Reagent Company. Na$_2$WO$_4$, Co(C$_2$H$_3$O$_2$)$_2$ and [Bmim]Cl were purchased from Sinopharm Chemical Reagent Company Limited. All reagents were used without further purification.

Preparation of synergists

CoW was synthesized according to the literature of Frank Walmsley[22]; 9.9-g (0.0300 mol) Na$_2$WO$_4$ was dissolved in water, and glacial acetic acid was added to keep the pH between 6.0 and 7.0. Then, 0.6-g (0.0025 mol) Co(C$_2$H$_3$O$_2$)$_2$ was dissolved in water with two drops of glacial acetic acid added. The Na$_2$WO$_4$ solution was heated until boiling, and the Co(C$_2$H$_3$O$_2$)$_2$ solution was added all at once. The solution was boiled for 3 hr, then HCl was added until pH reaches 3.0. Then, it was cooled to room temperature, and the undissolved solid was removed. Next, 2.6-g (0.0149 mol) [Bmim]Cl was added into filtrate, then CoW was obtained. It was a blue solid and cannot dissolve in water. Then, the CoW was washed by water for 10 times to further purify.

Preparation of PP composites

All the PP composites were prepared by melt blending on a Brabender mixer at 200℃ with rotation speed of 50 r/min for 10 min. The weight ratio of APP and PER mixture was 3:1. And the mixed materials were hot-passed into sheets in the dimensions of 100.0 mm × 100.0 mm × 3.2 mm by compression molding at 200℃ under 10 MPa for 3 min. The composites sheets were further cut into suitable bars for UL-94 and LOI testing.

Characterization

FTIR spectra were recorded with a Nicolet 6700 FT-IR spectrometer. Samples were mixed with KBr powders and compressed into wafers.

^{1}HNMR spectra were recorded with a 400-MHz AMX NMR spectrometer using DMSO-d$_6$ as solvent.

UL-94 tests were performed according to ASTM D3801 on an AG5100B vertical burning tester (Zhuhai Angui Testing Equipment Company, China). The samples used for the tests were 100.0 mm × 13.0 mm × 3.2 mm in dimension.

LOI tests were performed according to ASTM D2863-97 on a 5801 digital oxygen index analyzer (KunshanYangYi test Instrument Co., Ltd.). The samples used for the tests were 100.0 mm × 6.5 mm × 3.2 mm in dimension.

TGA were performed on a TGA/DSC1 Analyzer (Mettler Toledo International Inc., Switzerland) at a heating rate of 10℃/min from 50℃ to 800℃.

Cone calorimeter tests were performed on FTT0242—Standard Cone (Fire Testing Technology Limited., England) at 35 kW/m^2 heat flux.

SEM of char layers was observed by S4800 (Hitachi Corp., Japan) after coated with a thin layer of conductive gold.

RESULTS AND DISCUSSION

Characterization of CoW

The ^{1}H NMR spectrums of [Bmim]Cl and CoW are presented in Fig. 1. As for [Bmim]Cl, the peaks at $\delta = 0.8$ ppm, 1.2 ppm, 1.8 ppm and 4.2 ppm can be assigned to the protons on butyl. The peak at $\delta = 3.9$ ppm is attributed to methyl protons. And the peaks at $\delta = 7.9$ ppm, 8.0 ppm and 9.7 ppm are attributed to the protons on imidazole ring. These characteristic peaks are also found in the ^{1}H NMR spectrum of CoW. Additionally, the peaks of the protons on imidazole ring of CoW show an obvious chemical shift because of the electronegativity change of the anion. For example, the peak 8 of [Bmim]Cl is at $\delta = 9.7$ ppm, and the corresponding peak of CoW is at $\delta = 9.1$ ppm. This is because the lower electronegativity of CoW$_{12}$O$_{40}^{6-}$ leads the peaks of imidazole ring shift to higher field.

The FT-IR spectra of [Bmim]Cl, CoW are shown in Fig. 2. The typical bands of [Bmim]$^+$ are indicated; 3143–2873 cm^{-1} belongs to C—H stretching in the imidazole ring, 1571–1465 cm^{-1} belongs to imidazole ring stretching and 1168 cm^{-1} belongs to imidazole H—C—C and H—C—N bending. These characteristic peaks are also observed in the FT-IR spectrum of CoW. In addition, the strong absorption peaks of 948–935 cm^{-1}, W=O$_t$ (terminal oxygen); 881–875 cm^{-1}, W—O$_c$—W (corner sharing oxygen) and 773–752 cm^{-1}, W—O$_e$—W (edge sharing oxygen) are the characteristic peaks of CoW$_{12}$O$_{40}^{6-}$ [23,24]. XRF is also applied to investigate the content of Co and W, and the results are shown in Table 1. This result suggests that the metal in CoW is consistent with the theoretical prediction. Combining ^{1}H NMR spectrums, FT-IR spectra and XRF, it is proved that the target product has been synthesized successfully.

LOI and UL-94 tests

The results of LOI and UL-94 are displayed in Table 2. The LOI of pure PP is 17.6 and is not classified in the UL-94 test. The LOI of PP/IFR composite with 20 wt% IFR is 26.0; however, the UL-94 result is not satisfied. In order to get better flame retardant property, much more IFR is needed. With the addition of 19 wt% IFR and 1 wt% CoW, the sample could achieve the UL-94 V-0, and the LOI value rises to 28.8. The lowest combination of IFR and CoW to achieve the UL-94 V-0 is 16 wt% IFR and 1 wt% CoW (sample 5). The results show that CoW can improve the flame retardant property of PP/IFR composites evidently.
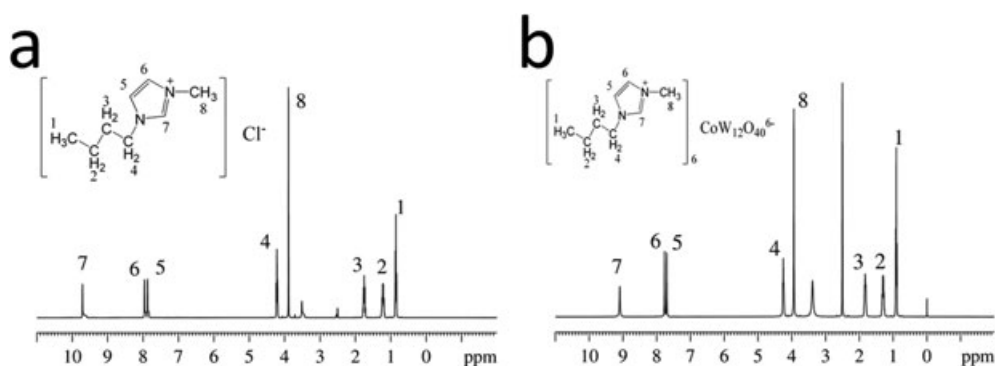
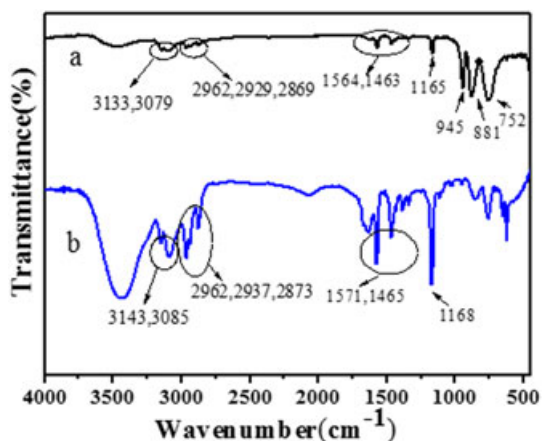**Figure 1.** ^{1}H NMR spectrums of (a) [Bmim]Cl and (b) CoW.

Figure 2. FT-IR spectra of (a) CoW and (b) [Bmim]Cl.

Table 1. XRF result of CoW

Sample	Co (wt%)	W (wt%)
CoW	96.8	2.4
Theoretical content of $CoW_{12}O_{40}{}^{6-}$	97.4	2.6

The influence of the catalyst content on the flame retardant property of PP composites is also investigated. Keeping the total content of IFR and catalysts as 17 wt% and adjusting the proportion of them, the LOI value increases first and then decreases with the content of catalyst increasing. The same phenomenon is obtained from the UL-94 test. The sample containing 1 wt% CoW is classified V-0 in the UL-94 test, while the other samples containing too much or too little CoW fail in the UL-94 V-0 test. Therefore, only a suitable content of catalyst can improve the flame retardant property.

The photos of the samples after LOI and UL-94 testing are shown in Figs 3 and 4. The sample 0 produces few char residues after the UL-94 and LOI test. With the addition of IFR, a little intumescent char is observed on the surface of the sample 3. When different amounts of CoW (from 0.5 wt% to 3 wt%) are added into PP/IFR composites (sample 4–7), the char residues for these samples after LOI testing are swelled, and their flame retardant properties are modified also. Especially, the sample 5 has the largest expanding volume and keeps good shapes after testing. Although the char residues for other samples look a little expansive, they fail in the UL-94 V-0 test. The detailed reasons will be researched in the following part. In addition, the color of sample 5 looks white or off-white, which is lighter than the reference [21] and shows broad application potential in the industry.

TGA of PP composites

The experimental (Exp.) and calculated (Cal.) TGA curves of PP, IFR, CoW and their blend system under N_2 atmosphere are

Table 2. Flame retardant properties of PP/IFR/CoW composites

Samples	PP (wt%)	IFR (wt%)	CoW (wt%)	UL-94	LOI (Vol%)	Melt dripping	t1 + t2 (sec)
Sample 0	100	0	0	NC	17.6	Y	/+0
Sample 1	80	20	0	NC	26.0	Y	0+/
Sample 2	80	19	1	V-0	28.8	N/N	0+0
Sample 3	83	17	0	NC	24.0	Y	0+/
Sample 4	83	16.5	0.5	NC	26.8	Y	0+/
Sample 5	83	16	1	V-0	28.0	N/N	0+0
Sample 6	83	15.5	1.5	V-1	28.6	N/N	0+13
Sample 7	83	14	3	NC	27.2	Y	0+/
Sample 8	85	14	1	V-1	27.0	N/N	0+13

Note: IFR is APP/PER = 3:1(wt%/wt%); NC means not classified in the UL-94 test.
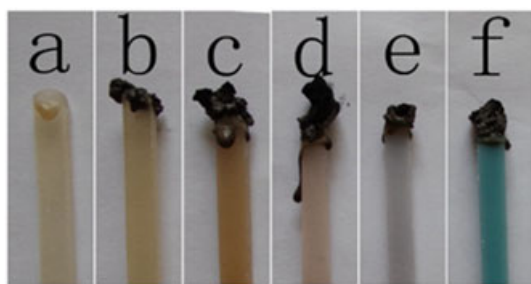
**Figure 3**. Photos of the samples after LOI testing: (a) sample 0, (b-f) samples 3-7.
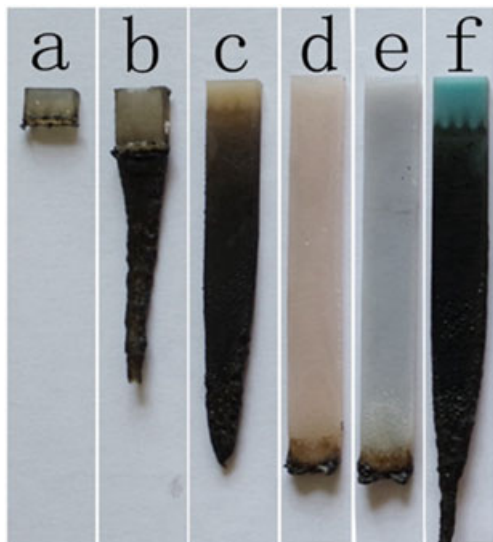
Figure 4. Photos of the samples after UL-94 testing: (a) sample 0, (b–f) sample 3–7.

shown in Fig. 5. The detailed data are listed in Table 3. The Cal. curves are calculated from the curves of IFR and CoW with their weight percentage (IFR: CoW = 16:1), PP and CoW (PP: CoW = 99:1), PP and IFR (PP: IFR = 83:17), PP, IFR and CoW (PP: IFR: CoW = 83:16:1), and the Exp. curves are the TGA results of their blend system. The temperatures at 1 wt%, 5 wt%, 10 wt% and 50 wt% degradation are noted as $T_{1wt\%}$, $T_{5wt\%}$, $T_{10wt\%}$ and $T_{50wt\%}$, respectively. The temperature at the maximum weight loss rate is noted as T_{max}.

The decomposition of IFR can be divided into three steps. According to the literatures [11–16], at low temperature range ($T < 280°C$), the APP decomposes and reacts with PER to form esters mixtures. At medium temperature range ($280°C \leq T \leq 350°C$), the esters would be swelled and forming the char layers because of the intumescent effect of the NH_3, which is produced from the decomposition of APP. At high temperature range ($T > 430°C$), the intumescent char layers decompose slowly, and part of the char structure is destroyed and loses foamed character. In addition, CoW shows good thermal stability. Its main degradation is at the temperature range from 350°C to 500°C. This is caused by the decomposition of organic moiety. The residue at 800°C is about 80 wt% meaning the content of inorganic part.

Comparing the Exp. and Cal. curves of IFR/CoW, the Exp. $T_{10wt\%}$ for IFR/CoW is 254°C, which is about 24°C lower than that of the Cal. One, indicating the early reaction of IFR promoted by CoW. As the temperature increases, the difference between the Cal. and Exp. degradation temperature under the same weight percentage increases first and then decreases gradually. For example, the Exp. $T_{5wt\%}$ for IFR/CoW is 209°C that is 30°C lower than the Cal. one, while the temperature gap for $T_{50wt\%}$ is only 2°C. Especially, the Exp. char residue at 800°C of IFR/CoW is enhanced obviously, which is 40.4 wt%, about 8.8 wt% higher than that of the Cal. one. These results suggest that the CoW has a significant influence on the thermal degradation behavior of IFR. It
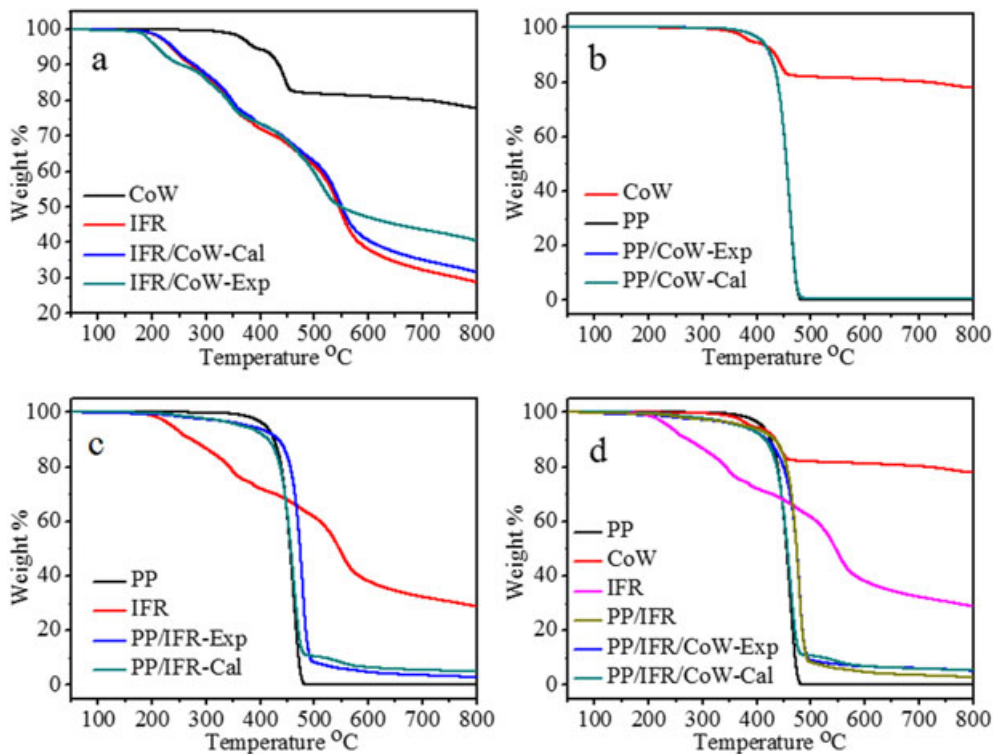

Figure 5. Exp. and Cal. TGA curves of (a) IFR/CoW, (b) PP/CoW, (c) PP/IFR and (d) PP/IFR/CoW under N_2 atmosphere.

Table 3. Exp. and Cal. TGA data of PP, IFR and CoW under N_2 atmosphere

Samples	$T_{1wt\%}$ (℃)	$T_{5wt\%}$ (℃)	$T_{10wt\%}$ (℃)	$T_{50wt\%}$ (℃)	T_{max} (℃)	Residues at 800℃ (wt%)
CoW	339	389	435	/	446	77.8
IFR	195	237	273	546	/	28.7
PP	364	410	426	455	461	0
IFR/CoW-Exp	179	209	254	549	/	40.4
IFR/CoW-Cal	197	239	278	551	/	31.6
PP/CoW-Exp	363	410	426	456	461	0.7
PP/CoW-Cal	364	410	426	456	461	0.7
PP/IFR-Exp	226	376	434	474	478	2.7
PP/IFR-Cal	241	365	414	457	462	4.8
PP/IFR/CoW-Exp	193	369	419	474	480	5.1
PP/IFR/CoW-Cal	243	370	416	457	462	5.3
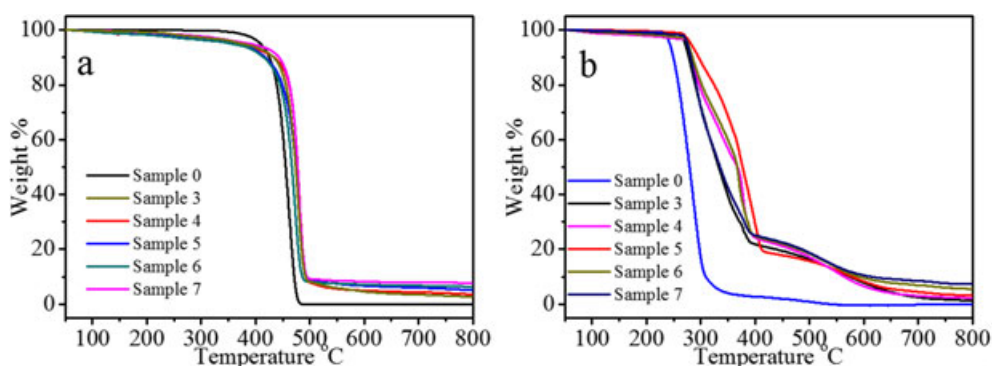
Figure 6. TGA curves of PP composites with different amounts of CoW: (a) under N_2 atmosphere, (b) under air atmosphere.

not only promotes the thermal degradation reaction of IFR at lower temperature, but also accelerates the char formation of IFR at higher temperature. More char layers can protect the underground resin from heat and gas, so the degradation behaviors after 549℃ are delayed.

Comparing the Exp. and Cal. curves of PP/CoW in Fig. 5(b), it is found that the Exp. curve fully coincides with the Cal. one. So CoW has few effects on PP during heating. The Cal. and Exp. TGA curves of PP/IFR are shown in Fig. 5(c). It is found that the Exp. curve of PP/IFR composite shifts to higher temperature comparing with the Cal. curve. Especially, the Exp. T_{max} of PP/IFR is 478℃, which is 16℃ higher than the Cal. one. The higher T_{max} reveals that the IFR is able to delay the thermal decomposition of PP composite, and has an obvious effect on thermal stability. In addition, the char residue of Exp. curve at 800℃ is 2.7 wt%, which is lower than the Cal. one. This means the quality of intumescent char layers is not good enough to prevent decomposition under high temperature.

The Cal. and Exp. TGA curves of PP/IFR/CoW composites are shown in Fig. 5(d). It is found that the Exp. curve of PP/IFR/CoW composite shifts to higher temperature. Its T_{max} is 480℃, 18℃ higher than that of the Cal. one, and 2℃ higher than PP/IFR. This indicates that the addition of CoW improves the thermal stability further. Additionally, the $T_{10wt\%}$ of PP/IFR/CoW is 419℃, 15℃ lower than that of PP/IFR. Its Exp. char residue reaches 5.1 wt%, which is 2.4 wt% higher than PP/IFR. Combining the results discussed above, it reveals that the synergistic effect exists mainly between IFR and CoW. Meanwhile, the addition of

CoW accelerates the thermal degradation reaction of IFR at lower temperature and promotes the char formation of IFR at higher temperature as well as the improvement of T_{max}.

The TGA curves of PP composites with different amounts of CoW under N_2 and air atmosphere are shown in Fig. 6. The detailed data are listed in Table 4. Under N_2 atmosphere, all samples show one-step degradation, and their curves shift to higher temperature with the addition of IFR. And the char residues have a significant increase after CoW is added. For example, the char residues at 800℃ of samples 4–7 are 3.6 wt%, 5.1 wt%, 6.3 wt% and 7.8 wt%, while that of sample 3 is only 2.7 wt%. These results reveal that CoW has good synergistic effect on the charring formation of PP/IFR composites under N_2 atmosphere. However, combining the LOI and UL-94 results, it is found that the sample which produces the most char residues does not obtain the best flame retardant property. This may be because of the char quality of the sample and will be discussed in the following.

Under air atmosphere, all the samples turn into a two-step degradation, and the flame retardants also make the TGA curves shift to higher temperature. In the first stage (270℃ ≤ T ≤ 400℃), the PP/IFR/CoW composites show better thermal stability than PP/IFR. In the second step(400℃ ≤ T ≤ 800℃), all the samples decompose slowly, and all PP/IFR/CoW composites produce more char residues than PP/IFR at 800℃. The T_{max} of samples 4–7 are 378℃, 403℃, 370℃ and 290℃, respectively, which are all higher than that of sample 3. It is worth noting that the T_{max} increases first and decreases gradually with the addition of CoW.

Table 4. TGA data of PP composites under N_2 and air atmosphere

Samples	N_2					
	$T_{1wt\%}$ (℃)	$T_{5wt\%}$ (℃)	$T_{10wt\%}$ (℃)	$T_{50wt\%}$ (℃)	T_{max} (℃)	Residues at 800℃ (wt%)
Sample 0	364	409	425	455	462	0
Sample 3	226	376	434	474	479	2.7
Sample 4	133	359	435	478	481	3.6
Sample 5	193	369	419	474	479	5.1
Sample 6	122	356	415	467	473	6.3
Sample 7	218	390	444	478	480	7.8
Samples	Air					
	$T_{1wt\%}$ (℃)	$T_{5wt\%}$ (℃)	$T_{10wt\%}$ (℃)	$T_{50wt\%}$ (℃)	T_{max} (℃)	Residues at 800℃ (wt%)
Sample 0	230	243	250	280	284	0
Sample 3	176	271	278	333	284	1.3
Sample 4	100	276	283	368	378	2.3
Sample 5	258	282	296	377	403	3.2
Sample 6	134	277	285	367	370	5.6
Sample 7	195	275	282	336	290	7.4
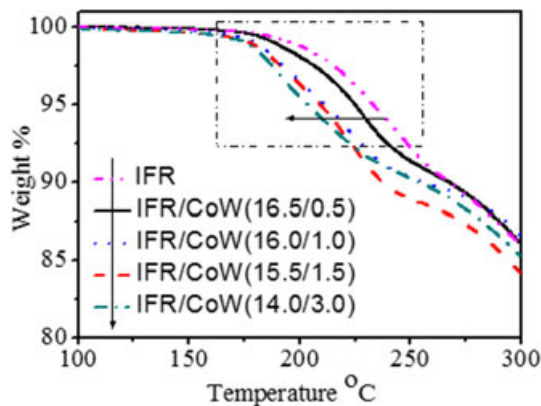
Figure 7. TGA curves of IFR with different amounts of CoW under air atmosphere.

Sample 5, which has the best flame retardancy, also gets the highest T_{max}. Additionally, the char residue of samples 4–7 increases from 2.3 wt% to 7.4 wt% with the content of CoW increase. These results reveal that CoW delays the thermal decomposition of PP/IFR composites and accelerates the char formation, but excessive CoW causes the degradation of IFR dramatically as shown in Fig. 6 (b) inside. So an appropriate amount of CoW is needed which is in accordance with the flame retardant properties.

In order to investigate the reaction between CoW and IFR, the thermal degradation behavior of IFR/CoW compounds with different amounts of CoW were studied and the results are shown in Fig. 7. The thermal degradation temperatures before $T_{10wt\%}$ are listed in Table 5. It is obvious that the degradation temperatures for IFR/CoW compounds decrease with the content of CoW increasing when the temperature is lower than $T_{7.5wt\%}$. For example, the $T_{5wt\%}$ of IFR is 233℃, while the $T_{5wt\%}$ of IFR/CoW compounds changes from 225℃ to 203℃. These results reveal that CoW accelerates the reaction of IFR, and improves its decomposition rate at early degradation stage. It is interesting that the IFR/CoW compound (14.0/3.0) obtains the most char residues. It suggests that even though excessive CoW accelerates the decomposition of IFR at early degradation, it also promotes the char formation at the later degradation stage because of the complexity of decomposition. Analyzing the results of flame retardant properties and thermal degradation, it also proves the same result. So the reason of excessive CoW causing the poor flame retardant properties may relate with the quality of char layer. In addition, the amount of sample for TGA test is so little that cannot present the real results absolutely. Therefore the rate of char formation at a larger sample quantity was studied.

Rate of char formation

According to the work reported by Edward D. Weil [25], the rate of char formation (RCF) is one of the most important

Table 5. TGA data of IFR with different amounts of CoW under air atmosphere

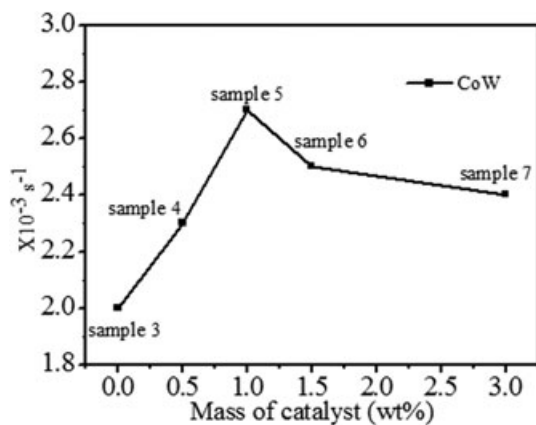| Samples	$T_{1wt\%}$ (℃)	$T_{5wt\%}$ (℃)	$T_{7.5wt\%}$ (℃)	$T_{10wt\%}$ (℃)	Cal. residues at 650℃ (wt%)	Exp. residues at 650℃ (wt%)
IFR	196	233	248	268	25.4	25.4
IFR/CoW(16.5/0.5)	189	225	239	267	27.1	34.0
IFR/CoW(16.0/1.0)	180	211	227	256	28.7	33.6
IFR/CoW(15.5/1.5)	177	209	223	237	30.4	32.0
IFR/CoW(14.0/3.0)	175	203	222	253	35.3	46.9

Figure 8. Rate of char formation.

factors for flame retardant performance of materials. Usually the materials which have higher RCF have better flame retardant properties as if the quality of char is good enough. The RCF is calculated from formulation (1), and the results are shown in Fig. 8.

$$RCF = m_c/(m_s*t) \qquad (1)$$

Here m_c means the weight of char residues; m_s means the weight of sample; t is burning time. The RCF of sample 3 is 2.0×10^{-3} sec^{-1}. When the amount of CoW increases from 0.5 wt% to 3 wt%, the RCF for these samples (samples 4–7) increases first and then decreases again. The sample 5 obtains the highest RCF, 2.7×10^{-3} sec^{-1}. This result reveals that CoW can promote the reactions between APP and PER, then enhance the RCF of PP composites. However, excessive addition of CoW will decrease the RCF. Although CoW accelerates the reaction between APP and PER, it also may promote the degradation of char. The two opposite effects result in different RCF and influence the flame retardant performance further.

CONE CALORIMETER TESTS

The flame retardant properties of PP composites were further studied by cone calorimeter. The time to ignition (TTI), heat release rate (HRR), total heat release (THR), mass loss (ML) and their peak values are shown in Fig. 9 and Table 6.

As shown in Fig. 9, PP burns severely in the testing, and its HRR curve is a single peak with a peak heat release rate (PHRR) of 1007 kW/m^2. Sample 3 and sample 5 turn into double peaks, the first peak is attributed to the protecting of the char layer and the second peak is attributed to the degradation of the char layer [26,27]. The PHRR for sample 3 and sample 5 are both lower than PP. With the addition of CoW, the PHRR of sample 5 is obviously delayed. It reaches PHRR at 357 sec, which is 52 sec later than sample 3. This may caused by the more char layers induced by CoW. The THR result is closely related to HRR. The THR of sample 0 is the highest one. Sample 5 shows the lowest THR. Its THR is 97 kJ/m^2 which is lower than sample 3 and sample 0. The ML results also have been studied in Fig. 9(c). Sample 0 burns severely and produces little char residue. The ML rate of sample 3 is lower, and the char residue is 18 wt%. With the addition of CoW, the ML rate decreases further, and the char residue reaches 20 wt%. These results indicate that CoW has a positive effect on PP/IFR system, promoting the char forming during combustion. The char layers protect the samples as a barrier, slow down the heat release and reduce the THR of composites.

MORPHOLOGY ANALYSIS OF CHAR RESIDUE

The photos of PP composites after cone calorimeter testing are shown in Fig. 10. There is little char for sample 0. With the addition of IFR, sample 3 produces a thin char layer which covers upon the whole substrate. However, an obvious crack can be observed at the center of the char layer for sample 3. So the quality and quantity of char layer are both unsatisfactory. And the low quality char layers cannot prevent the samples from the transfer of heat and combustible gases. When the CoW were added, a continuous and compact char layer is observed for sample 5.
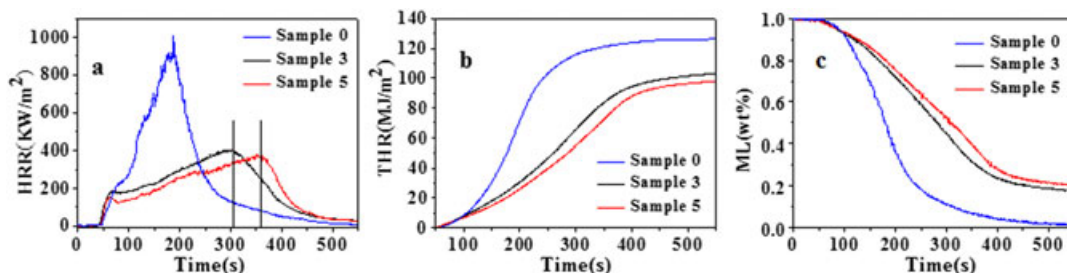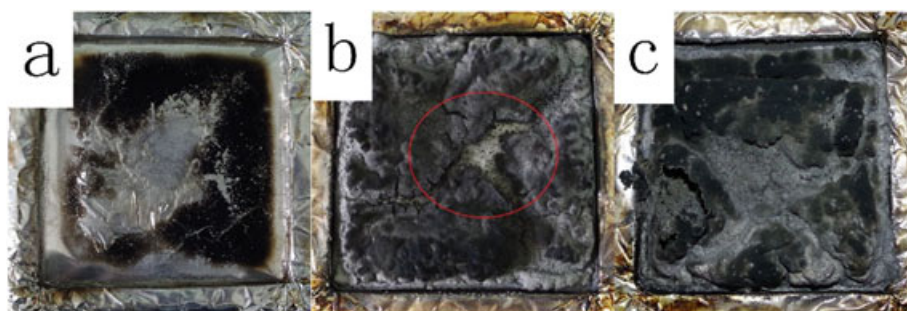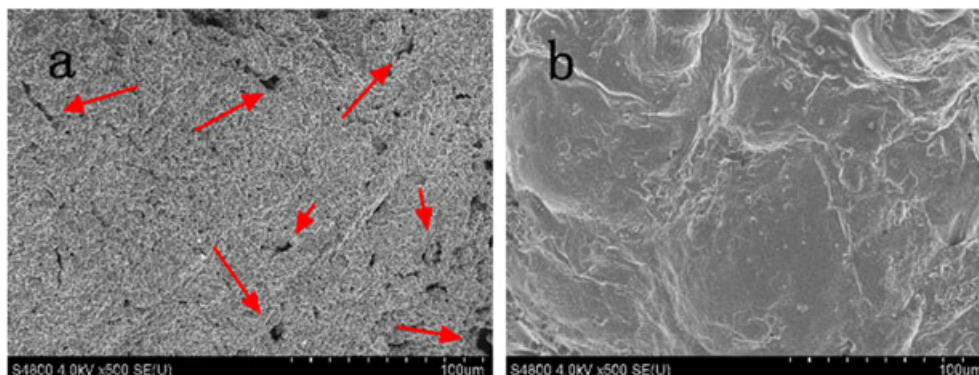

Figure 9. The cone calorimeter curves of PP composites: (a) HRR, (b) THR, (c) ML.
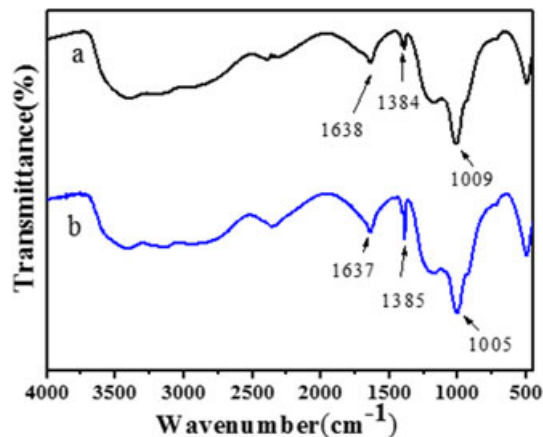
Table 6. Cone calorimeter data of PP composites					
Samples	TTI (sec)	PHRR (kW/m^2)	THR (kJ/m2)	Mean MLR (g/sec)	Char residues (wt%)
Sample 0	50	1007	126	0.104	0
Sample 3	46	402	103	0.030	18
Sample 5	46	401	97	0.030	20

Figure 10. Photos of PP composites after cone calorimeter testing: (a) sample 0, (b) sample 3 and (c) sample 5.

Figure 11. SEM photographs of char layers of (a) sample 3 and (b) sample 5.

Figure 12. FT-IR spectra of char layers for PP composites: (a) sample 3 and (b) sample 5.

This indicated that the quality of char layers has a huge promotion.

In order to investigate the morphology of the char layers for PP composites, the SEM photographs are shown in Fig. 11. There are many holes in the char layer of sample 3, indicating that the quality of char layer is unsatisfactory. However, few holes are observed in the char layer of sample 5. The compact char layer will protect the PP composites from heat and combustible gases as a barrier in the fire, and be swelled by the NH_3 which formed from IFR; then the insulation effect of heat enhanced further. This result indicates that the CoW brings an improvement to the quality of char layer, then elevates the flame retardancy of PP composites.

The FT-IR spectra of char layers are shown in Fig. 12. The typical bands of sample 3 belong to phosphoric or polyphosphoric, $3500–3000\,cm^{-1}$ belongs to OH, $1637–1638\,cm^{-1}$ belongs to C=C, $1384–1385\,cm^{-1}$ belongs to $\beta_{O—H}$ and $1005–1009\,cm^{-1}$ belongs to P—O [28]. These characteristic peaks are also observed in the FT-IR spectrum of sample 5. This indicates that the addition of CoW does not destroy the char structure. After analyzing the date comprehensively, it is known that CoW accelerates the char formation and modifies the quality of char layer, thus improving the flame retardant efficiency.

CONCLUSIONS

Co was chosen as a heteroatom to tailor the performance of polyoxometalates. A pale blue tungestocobaltic based organic–inorganic hybrid material, $[Bmim]_6CoW_{12}O_{40}$, was prepared successfully. The synergistic effect of CoW on flame retardancy of PP/IFR composites was studied. The results showed that the CoW improves the flame retardant properties of PP/IFR composites at a suitable content. Especially, at the total content of 17 wt % IFR/CoW (16:1), the sample passes the UL-94 V-0 testing, and the LOI value rises to 28.0. In addition, the color of PP composite is lighter that provides more potential applications. A certain amount of CoW accelerates the reactions between APP and PER at early degradation, promotes the char formation and enhances the quantity of char at high temperature. However excessive CoW will promote the decomposition of both IFR and char, and damage the char layer. It is the combination of good char quality, enough char residue and high RCF induced by CoW that results in the high flame retardant efficiency of PP/IFR composites.

REFERENCES

[1] X. L. Chen, J. Yu and S. Y. Guo, *J. Appl. Polym. Sci.*, *102*, 4943–51 (**2006**).

[2] W. L. Lee, L. C. Liu, C. M. Chen and J. S. Lin, *Polym. Adv. Technol.*, *25*, 36–40 (**2014**).

[3] M. L. Xu, Y. J. Chen, L. J. Qian, J. Y. Wang and S. Tang, *J. Appl. Polym. Sci.*, *131*, 8 (**2014**).

[4] Q. B. Tang, B. B. Wang, G. Tang, Y. Q. Shi, X. D. Qian, B. Yu, L. Song and Y. Hu, *Polym. Adv. Technol.*, *25*, 73–82 (**2014**).

[5] H. F. Zhu, J. Li, Y. K. Zhu and S. J. Chen, *Polym. Adv. Technol.*, *25*, 872–80 (**2014**).

[6] F. Salauen, G. Creach, F. Rault and X. Almeras, *Polym. Adv. Technol.*, *24*, 236–48 (**2013**).

[7] Y. Halpern, D. M. Mott and R. H. Niswander, *Ind. Eng. Chem. Prod. Res. Dev.*, *23*, 233–8 (**1984**).

[8] C. H. Ke, J. Li, K. Y. Fang, Q. L. Zhu, J. Zhu and Q. Yan, *Polym. Adv. Technol.*, *22*, 2237–43 (**2011**).

[9] W. Y. Chen, S. S. Yuan, Y. Sheng and G. S. Liu, *J. Appl. Polym. Sci.*, *132*, 8 (**2015**).

[10] X. S. Wang, H. C. Pang, W. D. Chen, Y. Lin, L. S. Zong and G. L. Ning, *ACS Appl. Mater. Inter.*, *6*, 7223–35 (**2014**).

[11] G. Gamino, L. Costa and L. Trossarelli, *Polym. Degrad. Stab.*, *7*, 25–31 (**1984**).

[12] G. Gamino, L. Costa and L. Trossarelli, *Polym. Degrad. Stab.*, *7*, 221–9 (**1984**).

[13] G. Gamino, L. Costa and L. Trossarelli, *Polym. Degrad. Stab.*, *6*, 243–52 (**1984**).

[14] G. Gamino, L. Costa and L. Trossarelli, *Polym. Degrad. Stab.*, *12*, 203–11 (**1985**).

[15] G. Gamino, L. Costa, L. Trossarelli, F. Costanzi and G. Landoni, *Polym. Degrad. Stab.*, *8*, 13–22 (**1984**).

[16] G. Gamino, L. Costa, L. Trossarelli, F. Costanzi and A. Pagliari, *Polym. Degrad. Stab.*, *12*, 213–28 (**1985**).

[17] J. S. Yi, H. Q. Yin and X. F. Cai, *J. Therm. Anal. Calorim.*, *111*, 725–34 (**2013**).

[18] D. D. Yang, Y. Hu, L. Song, S. B. Nie, S. Q. He and Y. B. Cai, *Polym. Degrad. Stab.*, *93*, 2014–8 (**2008**).

[19] Q. Wu and B. J. Qu, *Polym. Degrad. Stab.*, *74*, 255–61 (**2001**).

[20] Y. Liu and Q. Wang, *J. Appl. Polym. Sci.*, *107*, 14–20 (**2008**).

[21] S. J. Chen, J. Li, Y. K. Zhu, Z. B. Guo and S. P. Su, *J. Mater. Chem. A*, *1*, 15242–6 (**2013**).

[22] F. Walmsley, *J. Chem. Educ.*, *69*, 936–8 (**1992**).

[23] C. W. Hu, M. Hashimoto, T. Okuhara and M. Misono, *J. Catal.*, *143*, 437–48 (**1993**).

[24] E. Rafiee, M. Khodayari, M. Kahrizi and R. Tayebee, *J. Mol. Catal. A-Chem.*, *358*, 121–8 (**2012**).

[25] E. D. Weil, W. M. Zhu, N. Patel and S. M. Mukhopadhyay, *Polym. Degrad. Stab.*, *54*, 125–36 (**1996**).

[26] S. Bourbigot, M. LeBras, R. Delobel, P. Breant and J. M. Tremillon, *Polym. Degrad. Stab.*, *54*, 275–87 (**1996**).

[27] S. Bourbigot, M. Le Bras, S. Duquesne and M. Rochery, *Macromol. Mater. Eng.*, *289*, 499–511 (**2004**).

[28] A. N. Zheng, Y. Xia, N. Li, Z. W. Mao and Y. Guan, *J. Appl. Polym. Sci.*, *130*, 4255–63 (**2013**).

SUPPORTING INFORMATION

Additional supporting information can be found in the online version of this article at the publisher's website.